Proceedings Paper:
Uryga-Bugajska, I, Ma, L, Pourkashanian, M et al. (2008) Assessment of the performance of alternative aviation fuel in a modern air-spray combustor (MAC). In: ASME, (ed.) ASME 2008 International Mechanical Engineering Congress and Exposition (IMECE2008). IMECE2008, October 31 - November 6, 2008, Boston, Massachusetts. The American Society of Mechanical Engineers ., 61 - 69. ISBN: 978-0-7918-4864-7.

https://doi.org/10.1115/IMECE2008-68772

Proceedings of IMECE2008
2008 ASME International Mechanical Engineering Congress and Exposition
October 31 - November 6, 2008, Boston, Massachusetts

IMECE2008-68772

DRAFT: ASSESMENT OF THE PERFORMANCE OF ALTERNATIVE AVIATION FUEL IN A MODERN AIR-SPRAY COMBUSTOR (MAC)

Ilona Uryga-Bugajska
CFD Centre
University of Leeds
Leeds, LS2 9JT, UK

Mohamed Pourkashanian
CFD Centre
University of Leeds
Leeds, LS2 9JT, UK

Duncan Borman
CFD Centre
University of Leeds
Leeds, LS2 9JT, UK

Elena Catalanotti
CFD Centre
University of Leeds
Leeds, LS2 9JT, UK

Lin Ma
CFD Centre
University of Leeds
Leeds, LS2 9JT, UK

ABSTRACT

Recent concerns over energy security and environmental considerations have highlighted the importance of finding alternative aviation fuels. It is expected that coal and biomass derived fuels will fulfil a substantial part of these energy requirements. However, because of the physical and chemical difference in the composition of these fuels, there are potential problems associated with the efficiency and the emissions of the combustion process.

Over the past 25 years Computational Fluid Dynamics (CFD) has become increasingly popular with the gas turbine industry as a design tool for establishing and optimising key parameters of systems prior to starting expensive trials. In this paper the performance of a typical aviation fuel, kerosene, an alternative aviation fuel, biofuel and a blend have been examined using CFD modelling. A good knowledge of the kinetics of the reaction of bio aviation fuels at both high and low temperature is necessary to perform reliable simulations of ignition, combustion and emissions in aero-engine. A novel detailed reaction mechanism was used to represent aviation fuel oxidation mechanism. The fuel combustion is calculated using a 3D commercial solver using a mixture fraction/pdf approach. Firstly, the study demonstrates that CFD predictions compare favourably with experimental data obtained by QinetiQ for a Modern Airspray Combustor (MAC) when used with traditional jet fuel (kerosene). Furthermore, the 3D CFD model has been refined to use the laminar flamelet model (LFM) approach that incorporates recently developed chemical reaction mechanisms for the bio-aviation fuel. This has enabled predictions for the bio-aviation fuel to be made.

The impact of using the blended fuel has been shown to be very similar in performance to that of the 100% kerosene, confirming that aircraft running on 20% blended fuel should have no significant reduction in performance. It was also found that for the given operating conditions there is a significant reduction in performance when 100% biofuel if used. Additionally, interesting predictions were obtained, related to NO_x emissions for the blend and 100% biofuel.

INTRODUCTION

The advent of the 21st century has brought about significant issues for the commercial airline industry relating to the discharge of emissions. The international organisations responsible for setting emission levels of pollutants for the aircraft industry are continually setting ever more stringent standards [5, 6, 16]. This situation demands that the aircraft industry introduce new innovative technologies to improve engine performance and efficiency and that simultaneously cut emissions. One potential option is to utilise biofuels. From their conception, aircraft gas turbines have utilised kerosene as a basic aviation fuel. However, the concept of utilising alternative fuels in aircraft transportation has become a reality, as seen by the world's first commercial flight of an aeroplane with a biofuel-powered engine which took place on 24th February 2008.

Currently, biofuels are one of the direct substitute for oil available, on a large scale, that can be used in the transport sector in normal or slightly modified engines [7, 12, 19]. This is important since utilising existing engine technology significantly reduces the cost and time scales for implementation. Other technologies, such as hydrogen although important, need further development and their application on a wider scale is a considerable time away [3, 4, 12]. One of the main advantages of biofuels is that their use can produce significant savings in carbon dioxide emissions (so long as they are grown and processed in a sustainable way). Although they are not the cheapest way to cut emissions, biofuels provide a practical opportunity to make transport savings in the near future.

Using pure biofuels in aircraft engines is still a significant challenge since they have to satisfy all the engine application requirements. One of the drawbacks is the tendency for some biofuels to freeze at normal operating cruise temperatures and the poor high thermal stability characteristics [2, 4, 14]. The energy content of biofuel, which is influenced negatively by the presence of oxygen in the molecular structure, is relatively low when compared with that of conventional jet fuel. This means that the overall efficiency of the process is different. It can be concluded that when evaluating alternative fuels, factors such as their safety and their environmental effects must be considered as a priority.

In this study the performance of bio-aviation fuel represented by AFRMv2.0 is investigated in the MAC and is compared with the predictions for pure kerosene jet fuel which corresponds to AFRMv1.1 [9,11]. For this purpose a commercial 3D CFD solver is utilised. The combustion problem is solved using a range of different models. These are employed to solve differing phenomena within the combustor. The complexities of the flow field, which are influenced by turbulent fluctuations are resolved initially using a k-ε model and subsequently by the Reynolds Stress Model (RSM).

MODELLING APPROACH

Problem description

The MAC combustor has 22 rotational symmetry planes. Thus for the purposes of numerical modelling, only 1/22 of the total combustion chamber has been considered. A mesh created for this model consists of 198 000 hexahedral and 3600 prismatic wedge elements. The hexahedral mesh has been achieved by extruding the surface grid along the combustor, in the z direction, which allows us to produce a high quality mesh. Figures 2 (a) and (b) demonstrate the complete geometry and mesh of the airspray combustor in different views. In order to verify the quality of the mesh and to confirm the high accuracy of the CFD predictions, the original grid was adapted to the gradient of the temperature and mixture fraction. The final grid was composed of 851 000 nodes and it was found that the grid adaption did not produce superior results for temperature and velocity levels compared to those obtained with the coarser mesh. This strongly suggests that a mesh independent solution has been achieved.

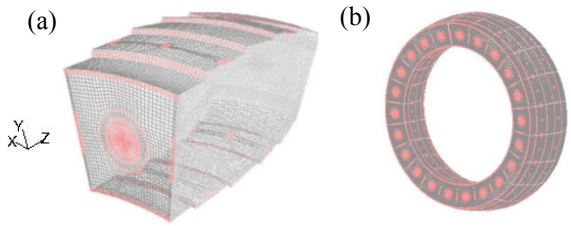

FIGURE 1 Geometry and mesh of the combustor: (a) - single burner port, (b) - full annular MAC geometry consisting of 22 burner ports.

The boundary conditions for the case have been provided by the QinetiQ and include profiles for the swirling air at the injector section and the mass flow for the remaining slots. A value of 700kPa was used for the operating pressure. The total mass flow of air and fuel was 12.815kg/s and 0.4746kg/s, respectively [9, 10]. Fuel entered the combustor via a thin annulus (5.6mm radius) at the centre of the injector in the same direction as air leaving the inner swirler, and was modelled as droplets with constant diameter 20µm and a temperature of 340K using Discrete Phase Model.

The cases listed in table 1 show the compositions of each of the three injected fuel mixtures[1]:

TABLE 1 Composition of each fuel mixtures used.

Case	Components	Fuel Composition (Mole %)
1. Pure kerosene	n-dekane $C_{10}H_{22}$ toluene -$C_6H_5CH_3$	89% 11%
2. Blend	Pure Kerosene Methyl Buthanoate (MB) - $C_5H_{10}O_2$	80% 20%
3. Pure biofuel	Methyl Buthanoate (MB) - $C_5H_{10}O_2$	100%

Alternative aviation fuel reaction mechanisms

A recent biofuel development, and now the most commonly used as a blend, is the fatty acid methyl ester (FAME). Produced by a process of trans-estrification of oils and fats with methanol, as described in figure 1, esters have similar chemical and physical properties to that of conventional diesel fuel [8].

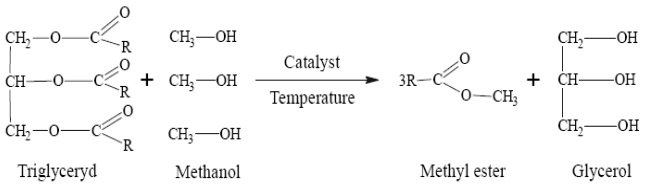

FIGURE 2 Reaction for vegetable oils methanolysis.

[1] Pure kerosene, blend and biofuel are represented respectively by: AFRM v1.1, AFRMv2.0, AFRMv2.0.

Bio aviation fuels are generally very large fuel molecules that challenge the capabilities of kinetic modeling. In addition, unlike traditional jet fuel FAME biodiesels contain around 11 percent of oxygen by weight [2]. This means biodiesel has a lower heating value compared with that of the same amount of conventional jet fuel (biodiesel: 36-39 MJ/kg; jet fuel: 43.2 MJ/kg). As such, there will be a reduction of power when directly replacing jet fuel with biofuel if no changes are made to the engine operating conditions. For this reason it would be necessary to increase the quantity of fuel injected into the combustor in order to produce the same power as that delivered using jet fuel.

In general the past research in this area has followed two major routes. Experiments and chemical kinetic modeling of much smaller methyl esters have addressed the special features of methyl ester oxidation. The high temperature oxidation of large biofuels has been studied by assuming that large methyl esters can be approximated as being fundamentally the same as large alkanes. A number of previous investigations focused on kinetic studies of methyl buthanoate, with a chain of only four carbon atoms connected to the methyl ester group.

A detailed chemical reaction mechanism AFRMv.2.0[2] describes in the paper by Catalanotti et al [3]; has recently been developed which can represent a number of different aviation fuels including bio aviation fuel. In this work we study its predictive performance for combustion within the MAC combustor. The results were compared against those of kerosene fuel modelled with AFRMv1.1[3] previously validated by Kyne et.al [9, 11] .

CFD Simulation methodology

Dealing with non-premixed turbulent flames requires a broad understanding of the system behaviour. As such, a detailed analysis is required before a suitable scheme can be selected to fully solve the problem. The difficulties are related to the complexity of the chemical kinetics and the strong non-linear connection between turbulence and chemistry. The turbulence-chemistry problem arises from the fact that generally the mixing process in combustion is slow when compared to the chemical reaction rates [21].

Due to the complexity of the problem certain modelling assumptions are made. In this study the Reynolds averaging (RANS) approach was chosen in order to resolve the turbulent flow. Two turbulence models were used: as a starting point the Standard k-ε (the first moment closure) was selected and then later the Reynolds Stress Model (RSM) was implemented because of its improved ability to predict swirling flows. The Reynolds Stress Model, also called the second moment closure model, is the most universal of all the classical turbulence models, since it provides very accurate predictions of mean flow properties. It can however, be significantly more time consuming than other models [1, 11].

[2] AFRMv.2.0 consists of 203 species and 116 reactions.
[3] AFRMv1.1 consists of 84 species and 440 reactions.

In order to solve the chemistry component of the process, the laminar flamelet model (LFM) was selected for its previously demonstrated accuracy in predicting turbulent combustion within an airspray combustor [9, 10]. The flamelet combustion definition is based on the principle that the reaction takes place in thin sheets that are nearby, and have similar structure to those of laminar flames. The LFM approach includes the local finite-chemistry effect, which results from turbulence influencing the thermo-chemical field [15, 17, 18]. The thermo-chemical condition is expressed by the conserved scalar quantity known as the mixture fraction f and a strain factor that is a scalar dissipation denoted by χ . The strain rate and scalar dissipation for the counterflow diffusion flamelet, can be described respectively as:

$$a_s = v/2d \quad (1)$$
$$\chi = 2D|\nabla f|^2 \quad (2)$$

Where a_s is the strain rate, v is the relative speed of the fuel and oxidizer jets, d is a distance between the jet nozzles and D represents the diffusion coefficient. For the each flamelet calculation, reaction mechanisms for pure kerosene, blend and pure biofuel were imported into Fluent along with a thermodynamic database to generate ten flamelet libraries each with a different scalar dissipation rate. The minimum value of χ was taken as 10^{-2} s^{-1} and the temperature and species mass fraction for further computation were obtained from the flamelet libraries.

In the non-premixed combustion regime, fuel and oxidizer enter the combustor as a two separate streams and the mixing of components occurs in the reaction zone. In order to solve this process the mixture fraction approach has been introduced into the model. Under a set of simplifying assumptions the instantaneous thermo-chemical state of the mixture is related to the mixture fraction *f*. The mixture fraction is the local mass fraction of the substances that originate from the fuel stream and in a system consisting of fuel and oxidizer it can be written as:

$$f = \frac{Z_i - Z_{i,ox}}{Z_{i,fuel} - Z_{i,ox}} \quad (3)$$

where Z_i is the elemental mass faction for element, *i*. The sum of the mixture fractions in the system for the fuel and oxidizer, must be equal to 1 (eq.4).

$$f_{fuel} + f_{ox} = 1 \quad (4)$$

This technique assumes the simplification of combustion to a mixing problem and the difficulties linked with the non-linear reaction rates are avoided. Data on the concentration of the species was obtained from the calculated mixture fraction fields in the pre-processor.

The turbulence-chemistry interaction was governed in this case by the assumed-shape probability Density Function (PDF), beta function, which has proven particularly useful [21] and offers the advantage that all the statistical information pertaining to the scalar field is embedded within the PDF.

The quantities of NOx found in the combustor are at trace levels and therefore will not influence the flow field significantly. This allows predictions for the thermal and prompt NOx species to be calculated within the NO_X model in the post processor, based on a steady-state solution of the calculated flow field. Thermal NO_x formation is determined by the extended Zeldovich reactions which are strongly dependant on temperature [13, 20 ,21].
In order to predict NO_x correctly, the partial equilibrium option has been assumed for the concentration of the O and OH radicals. It has been demonstrated that this approach provides satisfactory results at high temperature [21].

Experimental measurements

The experimental measurements for the combustion of kerosene within the MAC were made in five planes, at the following positions of the burner: Z=0.038m, Z=0.068m, Z=0.106m, Z=0.14m, Z=0.17m (where Z=0 describes a plane that passes through the injector nozzle). The experimental measurements were made within the MAC at 700kPa and with an overall Air to Fuel Ratio (AFR) =27. The full experimental setup is outlined in the paper by Kyne et al., 2002 [9, 10]. As experimental measurements did not demonstrate a symmetric pattern, both the left hand side (LHS) and the right hand side (RHS) of the burner locations have been considered (see black points on the temperature contour plots on fig. 5(a-c) in the results and discussion section). In order to verify theoretical predictions from CFD simulations and to compare with the five measurements points, a line perpendicular to the injector was selected (see figure 3). Since the periodic symmetry was assumed for the geometry, only one burner position was considered for the theoretical points.

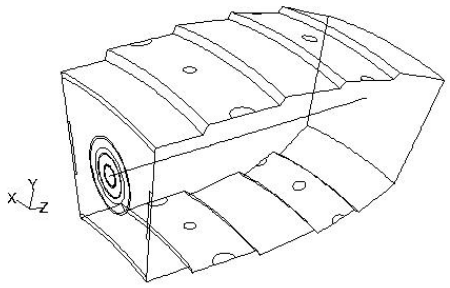

FIGURE 3 Theoretical measurements position.

RESULTS AND DISCUSSION

In this section the results of numerical simulations are presented for the three cases indicated in section 2.4. Previously outlined models have been verified by reproducing the conditions and predictions for the combustion of pure kerosene (conventional jet fuel) in the MAC combustor. These results are validated against the indicated experimental measurements provided by QinetiQ. Having validated the model for kerosene, the predictions for the further two fuel mixtures cases, where no empirical data is available, were then compared with the results obtained for the conventional aviation fuel.

In relation to the two turbulence models that were implemented, the Standard k-ε was found to be faster and demonstrated a higher level of stability than the RSM. However, the accuracy of simulation performed using RSM was significantly improved. For this reason the results outlined in the paper will focus on those produced using the RSM.

Comparison of the Combustion kinetics of the aviation fuels

The predictions for the temperature and mass fractions of CO_2, CO, O and OH using Opposed Flow Diffusion Flame (OPPDIF) calculations are shown in figure 4(a)-(c). This calculation was part of generating PDF tables for the laminar flamelet model in the CFD code. The dashed line (4a) denotes the position of the stoichiometric mixture fraction for the all fuels. As can be observed in Figure 4 (a) the maximum flame temperature is comparable for pure kerosene and blended fuel which occurs at mixture fraction $f_1 = 0.07$.
The same trend can be observed for the mass fractions of major and minor species such as O and OH (figure 4 b-c). Again, it has been found there is a quite good agreement between the pure kerosene and the blend case. This helps confirm that the impact of using 20% biofuel blended with 80% kerosene fuel on combustion chemistry is not significant. However, there is a significant variation on combustion chemistry when kerosene or blend fuels are compared with bio aviation fuel. The peak of the flame temperature (figure 4 (a)) is reached at mixture fraction $f_2 = 0.11$ and is slightly lower. From the combustion chemistry point of view those deviations can be attributed to differences in the properties of the biofuel compared with conventional aviation fuel. Due to the oxygen present in the methyl buthanoate molecule ($C_5H_{10}O_2$), with oxygen content typically 10% or greater by mass, bio aviation fuels will have an impact on the overall energy content of the fuel, air to fuel ratio and emission level. Together with the absence of any C–C bonds it is expected that during the oxidation process there will be low formation and high oxidation rates of particulates. It is expected that the bond energy for C-O bond fission (pyrolysis mechanism) is smaller than hydrogen abstraction (oxidation mechanism). Therefore the C-O bond breaks more easily than the C-H bond. Consequently, the pyrolysis mechanism may be more able to start the chain reaction at relatively low temperatures, which would result in the low ignition temperature. The physical delay of MB should be much shorter than that for many conventional fuels, resulting in a shorter total ignition delay which will have an impact on CO-CO_2 conversion process.

Theoretical chemical kinetics studied by the authors [3] shows that at high temperature MB in biofuel is consumed by hydrogen abstraction, with H atoms and $O^{\cdot}$, $H^{\cdot}$ radicals as the main contributors. Hydrogen abstraction from MB by H atoms is the most sensitive reaction as H atoms play a major role in

fuel consumption. However, at intermediate temperatures hydrogen abstraction, both by CH_3 radicals and H atoms, to consume MB play a more significant role.

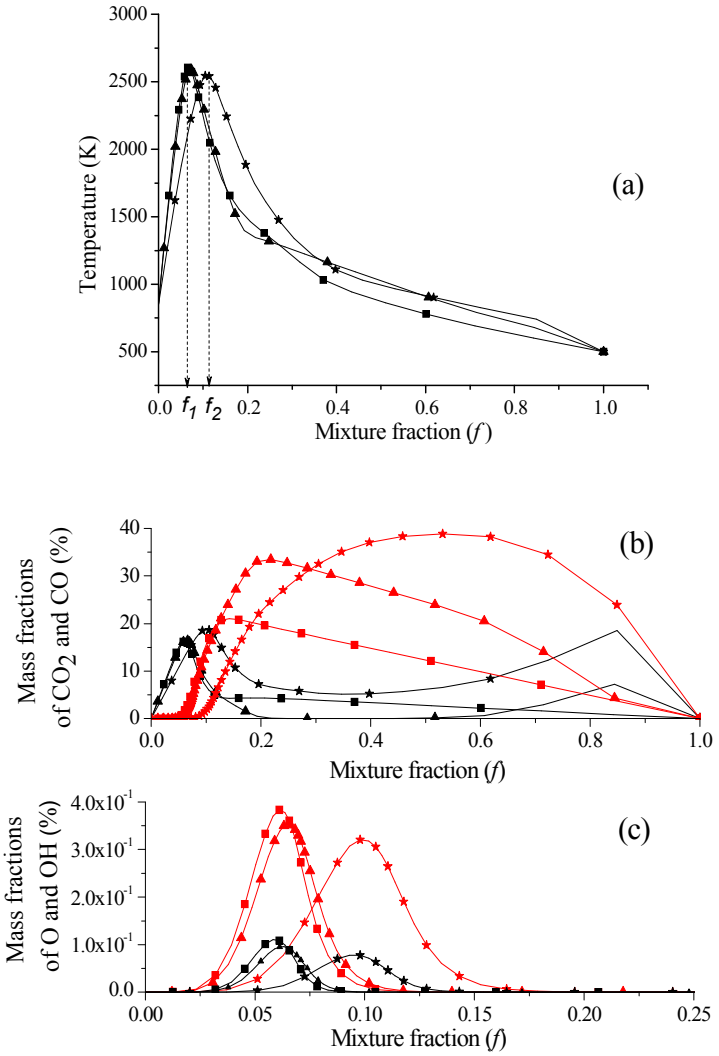

FIGURE 4 Flamelet calculations for the (a) - temperature; (b) - mass fraction of CO and CO_2 ; (c) mass fractions of O and OH respectively. Red lines on (b) and (c) plots represent the CO and O fractions; black lines on (a),(b) and (c) plots correspond to the temperature, CO_2 and OH respectively. Solid line and square, ■, : 100% of kerosene case; dashed line and triangle, ▲, : blend case; dotted line and star, ★, : 100% of biofuel case.

The oxygenated fuel may have an impact on CO to CO_2 conversion and this phenomenon should be investigated further especially in near the flame zone (rich combustion environment). The oxygenated fuel assists in the more complete combustion by providing oxygen, as part of the fuel molecule which partially explains the higher CO concentration within the flame area for the blend and biofuel (figure 4(b)).

Finally, bio aviation fuel has a low combustion enthalpy: lower than that of kerosene fuel due to the oxygen content of the molecules, which necessitates a larger fuel flow to the combustor in order to deliver the same amount of energy to that provided by kerosene. Further analysis of the combustion chemistry of the bio aviation fuels has been discussed by authors elsewhere [3, 22].

Discussion of the biofuels performance in comparison to kerosene fuel in the aero-engine combustion chamber

Contour plots of theoretical temperature predictions of this study using the flamelet model with a strain rate $100s^{-1}$ and a Reynolds stress turbulence model are shown in figure 5(f). Figures 5(a-e) show the contours of temperature at each of the measurements planes studied. A noticeable feature of the plots is that there is not the expected cyclic symmetry, leading to a similar distribution surrounding each of the burners. It was confirmed by the experimentalist that the influence of the side walls did not penetrate into the measurement zone and there was no damage to the combustor that could affect the temperature and species distributions. Figure 5(d) clearly shows the cooling created by the dilution air in reducing the temperature of hot gases before they reach the combustor exit. It is noticeable that the cooling effect downstream of the dilution air is significantly greater that the primary air (figure 5(b)). The predicted temperature profile for kerosene combustion in MAC combustors agree well with those of the experimental measurements. The hottest region appears towards the centre of the combustor (at around z=0.1).

The predicted temperature profiles for kerosene and blend are shown in figures 6 and 7. These combustor contour plots maintain very similar temperature profiles to one another throughout the combustor. Consequently, it may be concluded that there is little impact on the performance of the overall combustion characteristics when using 20% biofuel blended with kerosene. It is important to mention that the prediction do not take into consideration reduction of combustion enthalpy generated by replacing kerosene with 20% oxygenated fuel.

However, when comparing the predicted temperature profiles of Kerosene to the 100% biofuel combustion, figure 6 and 8, respectively, there is a significant difference between them. It is interesting to observe that in the case of the 100% biofuel that the flame volume moves closer to the fuel injector and therefore reduced ignition delay time. It is important to state that in this study the fuel flow rate remained constant for all fuels under investigation and therefore replacing kerosene with bio aviation fuel significantly reduces the combustion enthalpy. The significant reduction on the temperature profile is due to the dilution impact of the cooling stream. However, it is clear that pure biofuel combustion, will have a significant impact not only on efficiency of the overall system, such as the size of the fuel tank and the overall weight of the aircraft if combustion enthalpy remained constant.

Figure 9(a) demonstrates temperature profiles for all three cases and compares them to experimental measurements made for kerosene. As can be observed, for pure kerosene there is an excellent agreement for the exit temperature distribution.

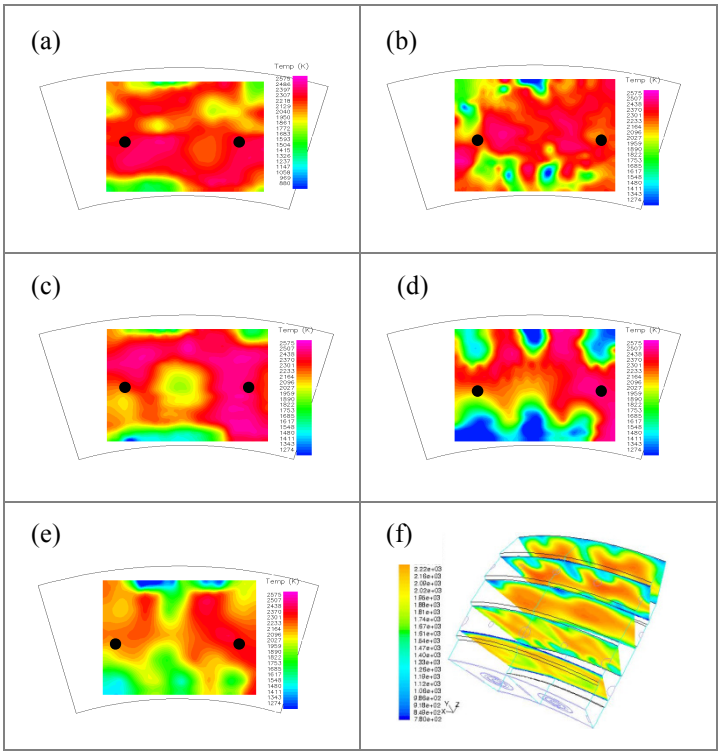

FIGURE 5 Temperature contour plots of experimental (a-e) and theoretical (CFD) predictions (f) for 100% kerosene.

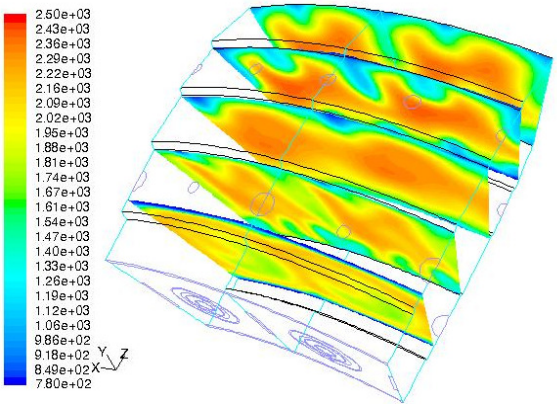

FIGURE 6 CFD predictions of temperature in the MAC combustor for the 100% of kerosene.

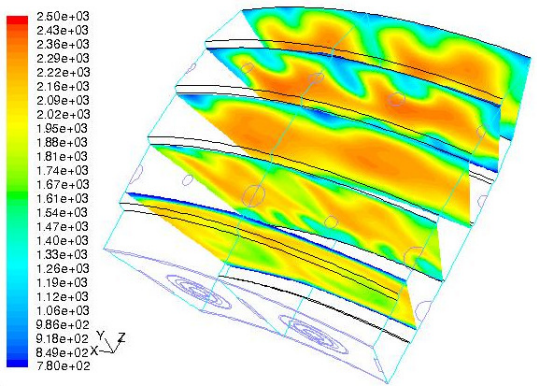

FIGURE 7 CFD predictions of temperature in the MAC combustor for the kerosene + biofuel blend (80:20).

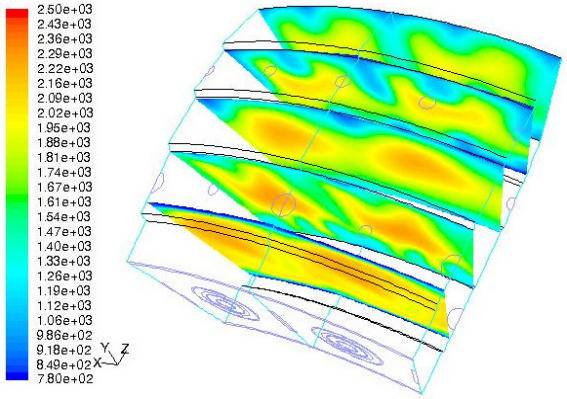

FIGURE 8 CFD predictions of temperature in the MAC combustor for the 100 % biofuel case.

Predictions for NO_x emissions

A primary interest for the CFD simulations was also to investigate the effect of fuel on NO_x formation route and emission levels in the exhaust. The NO_x profile in MAC combustor was computed with a partial equilibrium approach using the previously calculated temperature and species mixture fractions. Turbulence-chemistry interaction was modelled using a joint pdf approach using two statistically independent variables. It was observed that in both the kerosene and blend cases (figure 9(b-c)) that, as dictated by the extended Zeldovich mechanism, the majority of the NO_x formation occurs in the post-flame volume area where the gas temperature and OH/O concentration is high. The predicted NO_x formation results show that the predominant source of NO_x is from thermal, with prompt supplying less than 10%. As outlined in section 2.3, thermal is the dominant process for NO_x production at high temperatures (above 1800K) [21].

Figure 9(b) shows the mole fraction of NO_x found within the combustor for each fuel. It is clear that both kerosene and

blend show the correct trend of increasing NO_x with distance down the combustor injector centerline, however there is a noticeable under prediction in the rise of NO_x concentration. The flamelet model gave the closest agreement particularly in the exhaust region. The reactions used in the NO_x post processor that are responsible for the majority of NO_x are taken from the extended Zeldovich mechanism [21].

The 100% biofuel behaves notably different from the kerosene and blend as seen in figure 9(b). The early NO_x concentration is relatively high, but the quantities remain reasonably flat towards the exhaust, unlike the kerosene which shows an increase. It has been noted earlier that the temperature close to the injector is higher for 100% biofuel, this results in the formation of relative higher thermal NO_x at the injector. The temperatures for 100% biofuel are significantly lower in the second half of the combustor which leads to the reduction of thermal NO_x formation rate at the exhaust side.

In the case of the blend, the NO_x results are also noteworthy. It can been seen in figure 9(b) that there appears to be an increase in NO_x concentrations for the blend relative to the 100% kerosene. This can be better understood by considering both the temperatures profile in the combustor and the reactive minor species profile for each process.

It has been noted that the temperature profiles are similar in both cases with the blend becoming moderately hotter in the first half of the combustor and slightly cooler near the exhaust side (figure 9(a)). This small increase in temperature can only partially explain the increased NO_x.

The rate of NO_x formation for the blend close to the injector is increased as shown in figure 9(c). Overall it can be observed that there is a significant increase in the rate of thermal NO_x production close to the injector. At z=0.005, the rate of thermal NO is 0.003 and 0.0075, for kerosene and blend, respectively. This can be seen more clearly in the contour plots for NO_x rate of production for kerosene and blend in figure 10(a) and 10(b) respectively. These highlight the increased production of NO_x for the blend in the region close to the injector (signified by increased green and yellow on the first plane at z=0.005). It is anticipated that this phenomenon is primarily caused by the additional oxygen present in the molecular structure of the methyl ester molecule. Overall this change in the chemistry is responsible for the increased NO_x in the blended case, through moving the reaction zone towards the nozzle. Consistent with this, the rate of production reduces at the exhaust, and similarly the kerosene and blend mole fractions of NO_x in the combustor are observed to move closer together at the exhaust (figure 9(b)).

The proportions of production of prompt and thermal NO_x in the combustor can be observed in figure 11(a-d). Figure 11(a-b) show contour plots for thermal rate for kerosene and blend, respectively, whilst the figure 11(c-d) indicate the prompt NO_x rate of production for kerosene and blend, respectively. This indicates that there is also additional prompt NO_x formation in the blend close to the injector which also contributes to the relatively high total mole fraction of NO_x observed in figure 9(b).

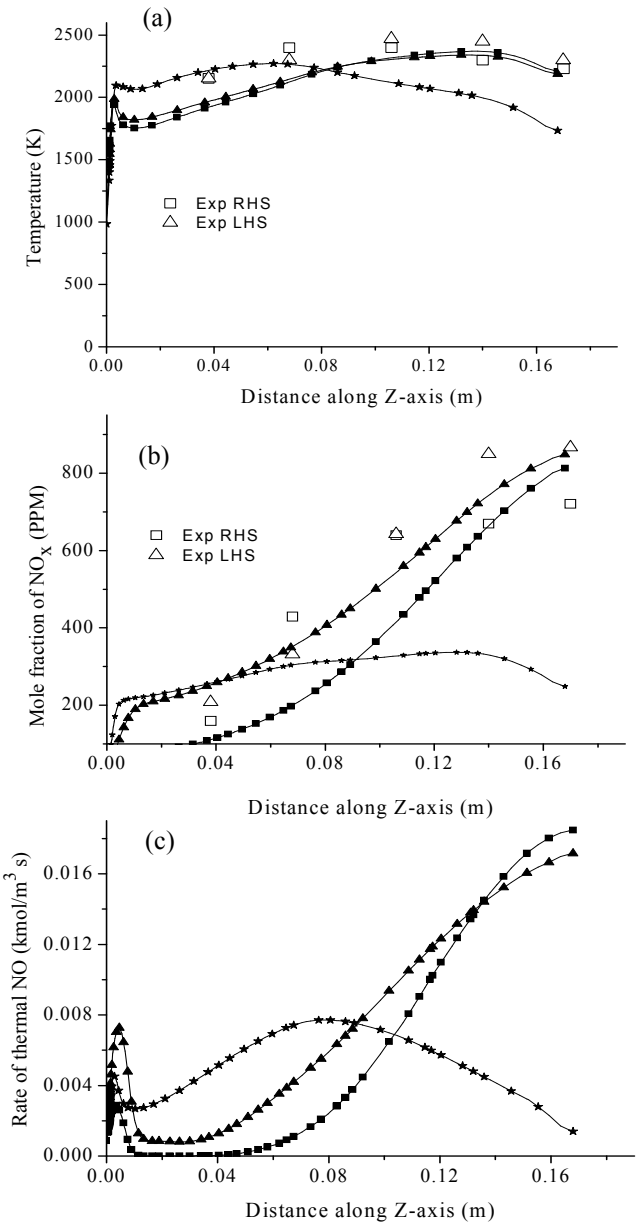

FIGURE 9 Comparison of experimental and CFD simulation temperature profiles (a), mole fraction of NO_x (b) and (c) rate of thermal NO formation for indicated fuel cases respectively. Empty squares and triangles, represents respectively experimental measurements for 100% of kerosene case taken from the left and right hand side (LHS), (RHS) of the burner. Solid line and square, —■—, : 100% of kerosene case; dashed line and triangle, —▲—, : blend case; dotted line and star, —★—, : 100% of biofuel case.

When investigating the NO_x emissions further it will be useful to calculate the emission index (EI) based on fuel enthalpy which will allow further analysis of the different fuel types based on normalising their energy content.

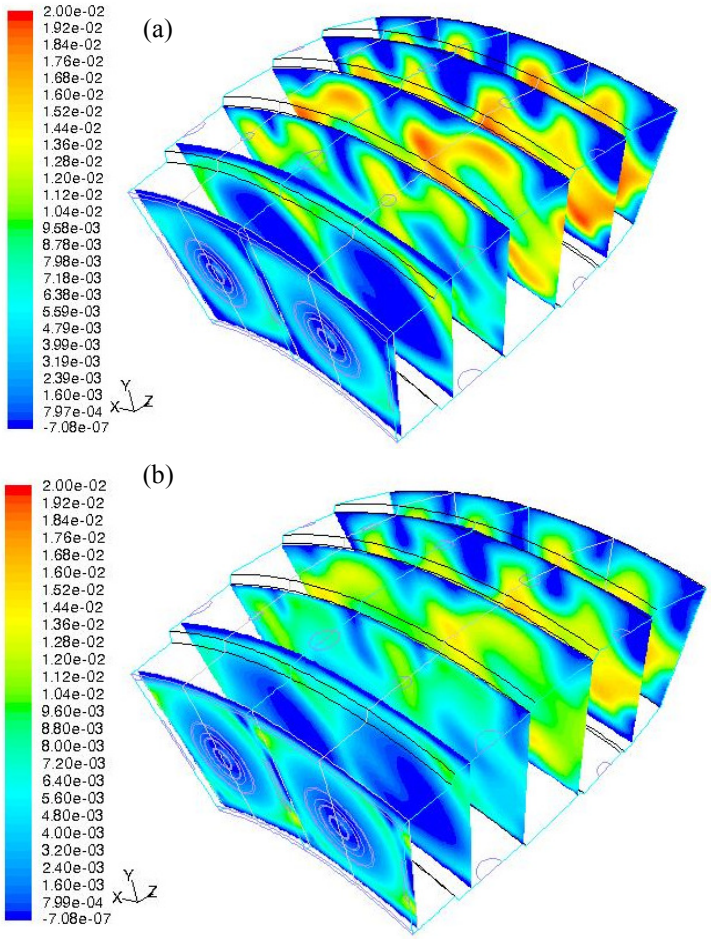

FIGURE 10 CFD predictions of rate of production NO (kgmol/m^{3}s) (a) for pure kerosene;(b) for the blended fuel, respectively.

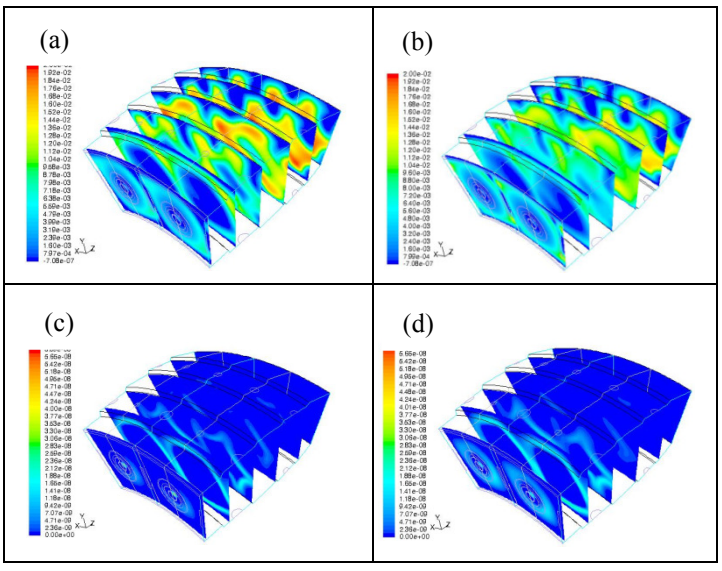

FIGURE 11 CFD predictions of rate of production (kgmol/m^{3}s) of thermal NO (a-b) and prompt NO (c-d) for kerosene and blended fuel, respectively.

SUMMARY AND CONCLUSIONS

In this paper the properties of a bio-aviation fuel have been investigated for a modern airspray combustor (MAC) using the recently developed detailed reaction mechanisms, AFRMv2.0, and a CFD simulation approach. The CFD predictions for kerosene were validated against experimental data from QinetiQ. The following conclusions can be drawn from the present study:

The impact of using the blended fuel has been shown to be very similar in combustion performance to that of the 100% kerosene.

The detailed reaction mechanism was validated against experimental data for kerosene and subsequently applied to blend and biofuel.

The predicted temperature and NO profile was in good agreement with the experimental values particularly at the exhaust.

Although at the exhaust, the amount of NO_x observed in the blended biofuel, was similar to that of kerosene, a substantially increased value was observed close to the injector. This phenomena is primarily attributed to the increased oxygen content of the methyl ester molecule which effects changes to the combustion chemistry close to the injector.

When using the 100% biofuel there is a significant impact to the performance of the process. At the operating conditions considered in this work, 100% biofuel would result in a significant reduction on combustion enthalpy.

In order to improve the reliance on the theoretical work, it is essential to carryout experimental work using blend and bio fuel for validation purpose.

ACKNOWLEDGMENTS

We wish to thank the European Union for financial support of Elena Catalanotti and Ilona Uryga-Bugajska as part of the Marie Curie FP6 Early Stage Training "Centre of Excellence in Computational Fluid Dynamics", contract MEST-CT-2005-020327.

NOMENCLATURE

Acronyms

AFRMv.1.1 = Aviation Fuel Reaction Mechanism(kerosene based)
AFRMv.2.0 =Aviation Fuel Reaction Mechanism (which includes biofuels chemistry)
LFM = Laminar Flamelet model
LHS = Left hand side of the burner
MB = Methyl Buthanoate
OPPDIF = Opposed Flow Diffusion Flame
RHS = Right hand side of the burner
RSM = Reynolds Stress Model
RANS = Reynolds averaged Navier Stokes

Symbols

a_s = strain rate
d = distance between the jet nozzles
D = diffusion coefficient

f = mixture fraction
f_1 = stoichiometric mixture fraction - 100% kerosene and blend
f_2 = stoichiometric mixture fraction - 100% biofuel
v = relative speed of the fuel and oxidizer jets
Z_i = elemental mass fraction for element, i

REFERENCES

[1] Bilger, R.W., 2000, "Future progress in turbulent combustion and research", Progress in Energy and Combustion Science, **26**, pp. 367-380.

[2] Canakci, M., 2005, "Performance and emissions characteristics of biodiesel from soybean oil" IMechE, part D: J. Automobile Engineering, **219**, pp. 915-919.

[3] Catalanotti, E., Hughes K.J., Pourkashanian M., Uryga-Bugajska, I., Williams, A., 2008, "Development of a high temperature oxidation mechanism for bio-aviation fuels". Draft version of the paper submitted to ASME International Mechanical Engineering Congress and Exposition, Boston.

[4] Daggett, D.L., Hendricks R.C., Walther R., Corporan E., 2007, "Alternate Fuel for use in Commercial Aircraft", The Boeing Company.

[5] Ebbinghaus, A., Wiesen, P., 2001, "Aircraft Fuels and their effect upon Engine emissions", Air & Space Europe, **3**, pp. 24-50.

[6] Federal Aviation Administration, 2007, "Aviation and the environment - managing the challenge of growth".

[7] Heminghaus, G., Boval, T., Bosley, C., Organ, R., Lind, J., Brouette, R., Thomson, T., Lynch, J., Jones, J., 2006, "Aviation Fuels Technical Review", Chevron.

[8] Heyl, A., Bockhorn, H., 2001, "Flamelet modeling of NO formation in laminar and turbulent diffusion flames", Chemosphere, **42**, pp. 449-462.

[9] Kyne, A.G., 2002, "Experimental and Theoretical Investigation of the Oxidation of Kerosene". University of Leeds PhD Thesis.

[10] Kyne, A.G., Porkashanian, M., Wilson, C.W., Williams, A., 2002, "Validation of a flamelet approach to modelling 3-D turbulent combustion within an airspray combustor". ASME Turbo Expo: land, sea and air.

[11] Leschinzer, M. A., 1990, "Modelling engineering flows with Reynolds Stress turbulence closure", Journal of Wind Engineering and Industrial Aerodynamics, **35**, pp. 21-47.

[12] Maurice, L.Q., Lander, H., Edwards, T., Harrison, III W.E., 2001, "Advanced aviation fuels: a look ahead via a historical perspective", Fuel, **80**, pp. 747-756.

[13] Miller, J.A., and Bowman, C.T., 1989, "Mechanism and Modelling of Nitrogen Chemistry in Combustion", Progress in Energy and Combustion Science, **115**, pp. 287-338.

[14] Mohibbe, A.M., Waris A., Nahar N.M., 2005, "Prospects and potential of fatty acid methyl esters of some non- traditional seed oils for use as biodiesel in India", Biomass and Bioenergy, **29**, pp. 293-302.

[15] Patterson, P.M., Kyne, A.G., Pourkashanian, M., Williams, A. and Wilson, C.J., 2001, "Combustion of Kerosene Counter-Flow Diffusion Flames", AIAA Journal of Propulsion and Power, **17(2)**, pp. 453-460.

[16] Penner, J.E., Lister, D.H., Griggs, D.J., Dokken, D.J. and Mcfarland, M., 1999, "Summary for Policymakers: Aviation and the Global Atmosphere", A special report of IPCC Working Groups I and III: Published for the Intergovernmental Panel Climate Change.

[17] Peters, N., 1984, "Laminar Diffusion Flamelet Models in Non Premixed Combustion", Progress in Energy and Combustion Science, **10**, pp. 319.

[18] Riesmeier, E., Honnet, S., Peters, N., 2004, "Flamelet modelling of pollutant formation in gas turbine combustion chamber using detailed chemistry for a kerosene model fuel", Journal of Engineering for Gas Turbine and Power (ASME), **126**, pp. 899-905.

[19] The European Commission, 2006, "Biofuels in the European Union. A vision for 2030 and beyond", Brussels.

[20] Tsague, L., Tsogo, J., Tatietse, T.T., 2006, "Prediction of the production of nitrogen oxide (NOx) in turbojet engines", Atmospheric Environment, **40**, pp. 5727-5733.

[21] Warnatz, J., Maas, U., Dibble, R.W., 2001, "Combustion. Physical and Chemical Fundamentals, Modelling and Simulation, Experiments, Pollutant Formation", Springer, Berlin.

[22] Dagaut, P., Gail, S., 2007, "Chemical kinetic study of the effect of a biofuel additive on Jet-A1 combustion", Journal of Physical Chemistry A, **111**, 3992-4000.